

*Biochimica et Biophysica Acta*, 466 (1977) 461–473  
© Elsevier/North-Holland Biomedical Press

BBA 77690

## THE PERMEABILITY OF ACONITINE-MODIFIED SODIUM CHANNELS TO UNIVALENT CATIONS IN MYELINATED NERVE

G.N. MOZHAYEVA, A.P. NAUMOV, Yu.A. NEGULYAEV and E.D. NOSYREVA

*Institute of Cytology, Academy of Sciences of the U.S.S.R., Leningrad, 190121 (U.S.S.R.)*

(Received October 18th, 1976)

### Summary

1. Ionic currents through the sodium system of nodes of Ranvier treated with aconitine were measured under voltage clamp conditions in a Ringer solution containing  $\text{Na}^+$  or an equimolar amount of various test cations.

2. Average shifts in reversal potentials in nodes of Ranvier treated with aconitine with  $\text{NH}_4^+$ ,  $\text{Li}^+$ ,  $\text{K}^+$ ,  $\text{Rb}^+$ ,  $\text{Cs}^+$  in place of  $\text{Na}^+$  in the Ringer solution are 7.6, -6.8, -25.0, -41.0 and -51.5 mV at 13–14°C. At 20–22°C the sequence of shifts is 7.5, -5.5, -13.5, -29.0 and -41.0 mV. For  $\text{Tl}^+$  the average reversal potential shift is +3 mV at 20–22°C.

3. The slope of the instantaneous current-voltage relation at the reversal potential in nodes treated with aconitine changed with the various cations tested. The ratios are  $\text{NH}_4^+/\text{Na}^+/\text{K}^+/\text{Rb}^+/\text{Cs}^+/\text{Li}^+ = 1.14 : 1.0 : 0.80 : 0.67 : 0.53 : 0.53$ .

4. Using a three energy barrier model some of the parameters for the aconitine-modified  $\text{Na}^+$  channels were estimated (Chizmadgeev, Yu. A., Khodorov, B.I. and Aityan, S.Kh. (1974) *Bioelectrochem. Bioenerg.* 1, 301–312).

---

### Introduction

Schmidt and Schmitt [2] showed that after the addition of the alkaloid aconitine to the Ringer solution bathing the node of Ranvier, a non-inactivating component of the inward current becomes apparent. This component reached a maximum near the resting potential of about -70 mV. For the other component both the kinetic and steady-state parameters were close to those of normal  $\text{Na}^+$ -channels. Both components however, exhibited a rather low reversal potential which was attributed to the accumulation of  $\text{Na}^+$  inside the fibre resulting from the steady-state inward current. This separation of the total inward current into two components was taken to indicate the existence of two types of channels in these membranes treated with aconitine.

Our recent study has supported this conclusion [3]. It turned out, however,

that the permeability of the channels, the kinetics of which were close to normal, decreases as aconitine effect develops and, eventually, disappears completely. At the same time the permeability of channels giving rise to a partly inactivating current component increases and attains a constant level.

The results presented in the previous study indicate that accumulation of  $\text{Na}^+$  during the sustained inward current after treatment with aconitine is not enough to explain the lowering of the reversal potential of the inward currents. The main cause of this phenomenon is that the selectivity of the channels is greatly reduced.

This decrease in selectivity caused by aconitine is likely to be associated with structural rearrangements in the channel. It would be of interest to study these rearrangements to disclose the nature of the selectivity. An important approach is the gathering of data on permeability properties of modified channels. In the present work the permeabilities of aconitine-modified  $\text{Na}^+$ -channels to  $\text{Na}^+$ ,  $\text{Li}^+$ ,  $\text{NH}_4^+$ ,  $\text{K}^+$ ,  $\text{Rb}^+$ ,  $\text{Cs}^+$  and  $\text{Tl}^+$  were estimated using conventional techniques.

## Materials and Methods

Single myelinated nerve fibres dissected from the sciatic nerve of *Rana ridibunda* were examined under voltage clamp conditions using the method developed by Nonner [4] with some modifications.

Fig. 1 shows the block diagram of the method used. The main modifications are: (1) Pool C, which is electrically connected with the input of feedback amplifier via special follower with the gain close to one (0.998–0.999) and very small virtual input capacity (about  $3 \cdot 10^{-14}\text{F}$ ), is surrounded by a screen connected to the output of the follower [5]. (2) Pool B is connected to the output of the follower and not to the ground. The first modification flattens

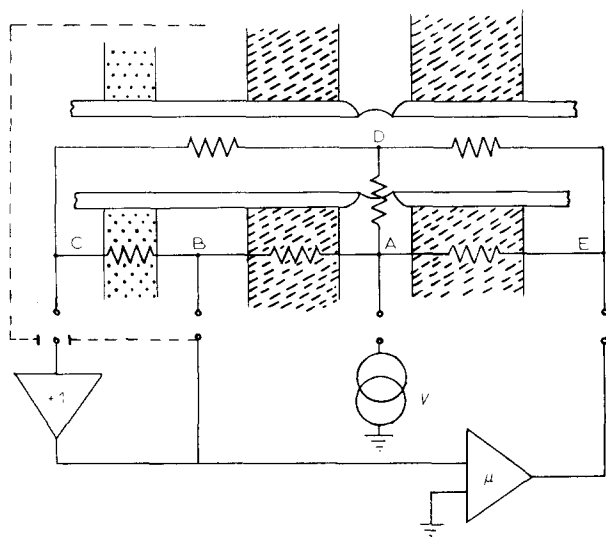


Fig. 1. Block diagram of voltage clamp. +1, follower;  $\mu$ , feedback amplifier, V, voltage source. Strocks denote vaseline; dots, air gaps.

the frequency gain characteristics of the preparation at frequencies within the range of physiological importance. This enables us to achieve the necessary time resolution (15–20  $\mu$ s) using standard solid operational amplifiers. The second modification makes screening of pool C easier, since pool B itself becomes a part of the screen. This method prevents the current from flowing over the surface of internode BC [6].

The nerve chamber was essentially as that described by Nonner [4]. AE, AC, AB-gaps are vaseline: BC is an air gap. Separations AE, AB, BC were set equal to 180, 150 and 70–100  $\mu$ m, respectively and these values were chosen to provide the stability of the nerve preparation and to exclude the “attenuation artifact” [7].

To check the “attenuation artifact” we compared the experimentally measured shift in reversal potential of the early current when the external concentration of sodium was reduced from 110 to 22 mM with the theoretically expected Nernst change. The average experimental value (four experiments) was  $-40 \pm 1.8$  mV, whereas the theoretically expected change at 14°C is  $-39.8$  mV. Thus our method effectively removes the “attenuation artifact”.

Membrane voltage ( $E_m$ ) is referred to the outside voltage. To estimate the membrane currents ( $I_m$ ) we assumed that the resistance of the axoplasm between points E and D was equal to 20 mohm.

Membrane currents were corrected for leakage by linear extrapolation of currents associated with hyperpolarizing voltage steps. The correctness of such method in some instances was supported by the observation that in the presence of  $10^{-7}$  M tetrodotoxin in external solution (in addition to 10 mM tetraethylammonium outside and 20 mM tetraethylammonium at cut ends of the fibre) the size of the remaining current was similar to that estimated using the hyperpolarizing pulse. When measuring currents associated with depolarizing voltage steps, we subtracted the capacity currents in the same manner as leakage currents. However, when “instantaneous” currents were measured, capacity currents were subtracted using a different method (see Results) since it has been observed that the value and time course of capacity current depends on membrane conductance.

The control Ringer solution (called Na<sup>+</sup>-Ringer) contains 110 mM Na<sup>+</sup>, 2 mM Ca<sup>2+</sup>, 5 mM Tris<sup>+</sup>, 10 mM tetraethylammonium<sup>+</sup>, 119 mM Cl<sup>-</sup>, 10 mM Br<sup>-</sup>. In the test solution (called K<sup>+</sup>-Ringer, Li<sup>+</sup>-Ringer, 0.5 Na<sup>+</sup>-Ringer etc.) the whole NaCl is replaced by an equimolar amount of the test salt or some of the NaCl is replaced by choline chloride. The ions tested are: NH<sub>4</sub><sup>+</sup>, K<sup>+</sup>, Rb<sup>+</sup>, Cs<sup>+</sup>, Li<sup>+</sup>, Tl<sup>+</sup>. Tl<sup>+</sup>-Ringer and Na<sup>+</sup>-Ringer for this comparison were made using nitrate salts. When necessary, Na<sup>+</sup>-Ringer with  $10^{-4}$ – $10^{-5}$  g/ml aconitine chloride or with  $10^{-7}$  M tetrodotoxin was used. pH of all solutions was adjusted to 7.3–7.4.

The ends of the fibres in pools C and E were cut in a solution containing 100 mM KF and 20 mM tetraethylammonium-bromide. Diffusion of the tetraethylammonium<sup>+</sup> from the cut ends towards the nodal membrane [8] compensates for the decrease in potency of the blocking effect of external tetraethylammonium when the membrane potential is made very positive during the pulses [9].

The experiments were carried out at 13–14°C and 20–22°C.

At the beginning of the experiments peak currents in  $\text{Na}^+$ -Ringer were measured with the holding potential ( $E_h$ ) set at  $-90$  mV. After this control the  $\text{Na}^+$ -Ringer was substituted by  $\text{Na}^+$ -Ringer with aconitine. To make sure that we were working with a stable population of modified channels it was necessary to make sure that: (1) the partly inactivating component of the current reached a maximum and constant (at any particular potential) level; (2) the inactivating component behaving as the expected for the normal  $\text{Na}^+$ -conductance had disappeared [3].

It has been noticed that development of the effect is speeded up considerably by periodical depolarizations of the membrane. Therefore, after the application of  $\text{Na}^+$ -Ringer with aconitine, a series of depolarizing pulses at a frequency of 10 per s was applied. The amplitude of these pulses was such that a small early outward current was seen. Under such conditions, the effects of aconitine developed completely in 2–3 min, while otherwise this process took 20–30 min [2,3].

To prevent the accumulation of  $\text{Na}^+$  inside the fibre (due to steady-state inward  $\text{Na}^+$ -current through modified channels) the holding potential  $E_h$  was increased to  $-110$ – $-120$  mV.

As the effect of aconitine is irreversible after producing the effects it was not applied together with the test solutions.

A further series of measurements of ionic currents was carried in  $\text{Na}^+$ ,  $\text{K}^+$ , Ringers, etc. To test for changes in the ionic composition inside the fibre during the experiment we measured the reversal potential  $E_r$  in the test solutions and in  $\text{Na}^+$ -Ringer. If the reversal potential in  $\text{Na}^+$ -Ringer differed from the initial value by more than 3 mV, results of subsequent measurements were discarded.

## Results

Fig. 2 shows tracings of the currents in modified  $\text{Na}^+$ -channels. It may be seen that having reached a peak value, ionic currents decayed towards a steady-state level with a time constant which becomes shorter with increasing the amplitude of the depolarizing pulse.

Fig. 3 shows the peak current-voltage relations for a node before and after treatment with aconitine.

One may distinguish the following differences in the current-voltage curves in Fig. 3. First, as compared to peak current-voltage relations for normal channels, those for modified channels are shifted to more negative potentials by approximately 30–40 mV. Second,  $E_r$  for the  $\text{Na}^+$ -current through modified channels has a lower value than  $E_r$  for normal  $\text{Na}^+$ -current. Since  $E_h$  was held at a level of  $-110$  mV, accumulation of  $\text{Na}^+$  was essentially excluded in these measurements. Thus the reduction of  $E_r$ , which in this case is equal to  $-37$  mV, must be caused primarily by differences in the selectivity properties of normal and modified channels. The slope conductance in  $\text{Na}^+$ -Ringer near  $E_r$  amounts to 35% of the corresponding value before the application of aconitine. In other experiments the slope conductance varied from 32 to 100% and averaged  $49 \pm 6\%$ . Such large scattering is apparently due to variations in the number of conducting channels. Part of the channels after treatment with aconitine turns to non-conducting state [3].

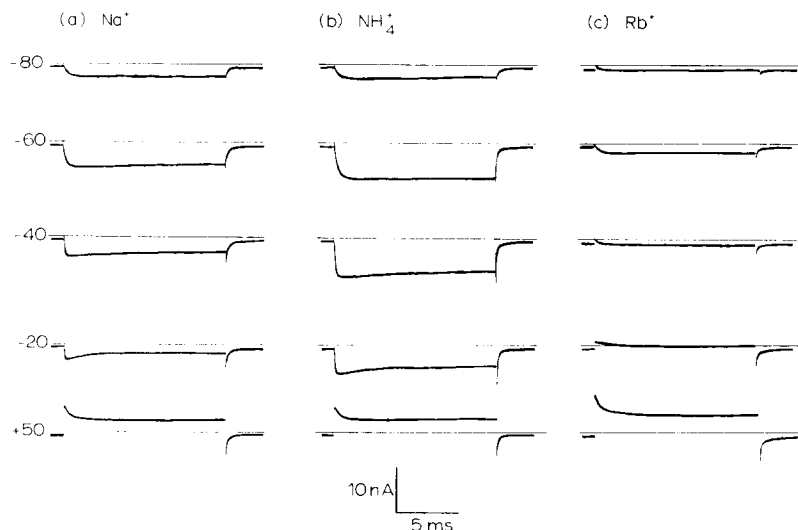


Fig. 2. Voltage clamp currents for a node treated with  $10^{-4}$  g/ml aconitine. (a) in  $\text{Na}^+$ -Ringer, (b) in  $\text{NH}_4^+$ -Ringer, (c) in  $\text{Rb}^+$ -Ringer. Membrane potential during pulses is indicated on the left. Thin line denotes zero current.  $E_{\text{H}} = -110$  mV. Currents are not corrected for leakage and a capacity. Node 37, temperature =  $14^\circ\text{C}$ .

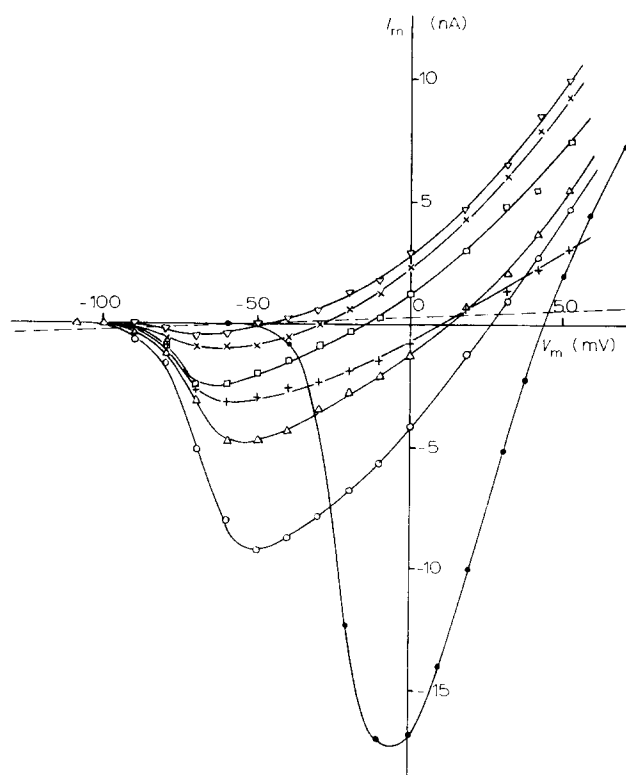


Fig. 3. Peak current-voltage relations for a node before (filled circles) and after (symbols in the inset) treatment with  $10^{-4}$  g/ml aconitine. Only one in  $\text{Na}^+$ -Ringer is shown (see Materials and Methods). Currents corrected for capacity and leakage. Leakage current is denoted by dashed line. Node 37, temperature =  $14^\circ\text{C}$ .  $\circ$ ,  $\text{NH}_4^+$ ;  $\Delta$ ,  $\text{Na}^+$ ;  $+$ ,  $\text{Li}^+$ ;  $\square$ ,  $\text{K}^+$ ;  $\times$ ,  $\text{Rb}^+$ ;  $\nabla$ ,  $\text{Cs}^+$ .

A widely used experimental criterium on channel selectivity is the measurement of reversal potentials of  $E_r$  (shifts in  $E_r$  ( $\Delta E_r$ ) produced by ionic substitution [10–12]).  $\Delta E_r$  values obtained in 17 experiments in which  $\text{NH}_4^+$  or  $\text{Li}^+$  or  $\text{K}^+$  or  $\text{Rb}^+$  or  $\text{Cs}^+$  were used in place of  $\text{Na}^+$  are presented in Table I. They were determined from both the current-voltage relations (as shown in Fig. 3) and from instantaneous current voltage relations (see below).

The partial inactivation of currents in modified channels seen in Fig. 2 suggests that there are two populations of channels with different inactivation properties. Fig. 4 shows both the peak and the steady-state current-voltage relations for a node in  $\text{Na}^+$ - and  $\text{NH}_4$ -Ringer. It is seen that  $E_r$  for both the peak and steady-state relation is the same in both solutions. This result indicates that all modified channels have the same selectivity.

Caesium ions are the least permeable of the cations tested in these modified channels.  $\text{Cs}^+$ -Ringer in place of  $\text{Na}^+$ -Ringer causes the greatest  $\Delta E_r$ . However, even the maximum value of  $-60$  mV (obtained in the experiment presented in Fig. 3) is considerably smaller than that for normal  $\text{Na}^+$ -channels (minimum,  $-104$  mV [12]). Thus, modified channels exhibit an appreciable  $\text{Cs}^+$  permeability. Inward current carried by  $\text{Ca}^{2+}$  may be neglected, if for no other reason than the much lower external calcium concentration.

An interesting observation is that  $\Delta E_r^{\text{Cs}}$ ,  $\Delta E_r^{\text{Rb}}$ ,  $\Delta E_r^{\text{K}}$  are smaller at  $20$ – $22^\circ\text{C}$  than at  $13$ – $14^\circ\text{C}$  by  $9$ – $12$  mV (see Table I).

TABLE I

THE SHIFTS IN REVERSAL POTENTIAL ( $\Delta E_r^i$ ) FOR NODES TREATED WITH ACONITINE ASSOCIATED WITH SUBSTITUTIONS OF  $\text{Na}^+$  IN THE RINGER SOLUTION BY A TEST CATION

Expt.	Temp. ( $^\circ\text{C}$ )	$\text{NH}_4^+$ (mV)	$\text{Li}^+$ (mV)	$\text{K}^+$ (mV)	$\text{Rb}^+$ (mV)	$\text{Cs}^+$ (mV)
15 *	21		-10	-15	-32	-47
27 *	22	+10	-5	-17	-23	-42
30 *	22	+9	-3	-13	-32	-40
33 *	20	+6			-25	
45 **	20				-30	
47 **	20		-2	-11		
49 **	21		-9			
51 **	22	+7	-3			
53 **	21	+7	-6	-16	-34	-41
54 **	21	+6	-10	-11	-25	-36
55 **	21		-2	-12	-29	-38
Mean $\pm$ S.D.		$7.5 \pm 1.6$	$-5.5 \pm 3.4$	$-13.6 \pm 2.4$	$-28.8 \pm 4$	$-40.7 \pm 3.8$
35 *	13	+4	-12			
36 *	13	+14	-9	-24		
37 *	14	+13	-3	-27	-42	-60
50 **	14	+4	-2		-39	-45
60 **	14		-5	-27	-38	-50
61 **	14	+3	-10	-23	-46	-51
Mean $\pm$ S.D.		$7.6 \pm 5.4$	$-6.8 \pm 4.0$	$-25.2 \pm 2.0$	$-41.2 \pm 3.6$	$-51.5 \pm 6.2$

\* Peak current-voltage relations.

\*\* "Instantaneous" current-voltage relations.

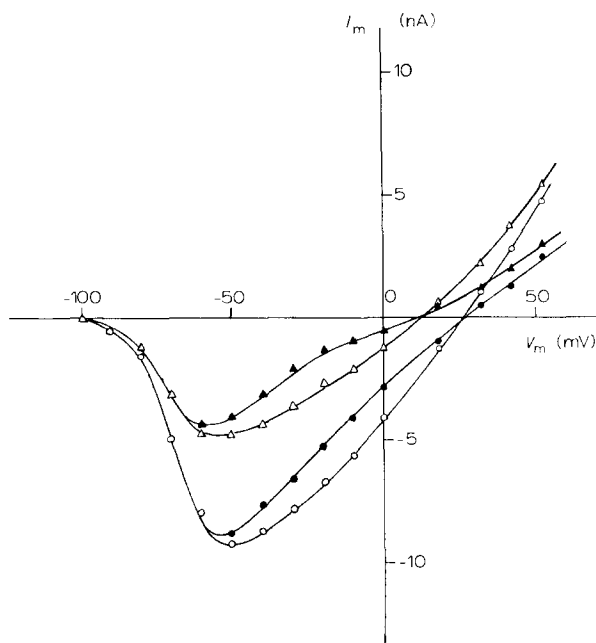


Fig. 4. Peak and steady-state current-voltage relations for a node treated with  $10^{-4}$  g/ml aconitine bathed in  $\text{Na}^+$ -Ringer (triangles) and in  $\text{NH}_4^+$ -Ringer (circles). Open symbols, peak currents; filled symbols, steady-state currents. Currents corrected for leakage and capacity. Node 37, temperature =  $14^\circ\text{C}$ .

The experiments with  $\text{K}^+$ -Ringer in place of  $\text{Na}^+$ -Ringer supported conclusions of previous work [3] that the  $\text{K}^+$ - $\text{Na}^+$  selectivity of the modified channels is greatly reduced. The average  $\Delta E_r^{\text{K}}$  at  $20$ – $22^\circ\text{C}$  is  $-13.5$  mV.

$\text{NH}_4^+$  is the most permeable cation through modified channels. The substitution of  $\text{Na}^+$ -Ringer by  $\text{NH}_4^+$ -Ringer causes a shift of  $E_r$  towards more positive membrane potentials.

The permeability of  $\text{Ti}^+$  in modified channels is close to that of  $\text{NH}_4^+$ . In the majority of the experiments  $\text{Ti}^+$  caused either an increase in leakage conductance and membrane breakdown, or the appearance of large and long symmetrical exponentially decaying currents. In two experiments, however, it was possible to obtain ionic currents in  $\text{Ti}^+$ -Ringer and the current-voltage relations are shown in Fig. 5.  $\Delta E_r^{\text{Ti}}$  in both cases was  $+3$  mV.

It may be seen in Fig. 3 that the substitution of  $\text{Na}^+$ -Ringer by  $\text{Li}^+$ -Ringer causes a considerable reduction in the slope of the current-voltage curve while  $\Delta E_r^{\text{Li}}$  is small. It should be noted, also, that after replacement of  $\text{Li}^+$ -Ringer by  $\text{Na}^+$ -Ringer the inward and outward currents were recovered slowly (5–10 min) and not immediately as with other ions. Such an effect may be connected with the penetration of the fibre by  $\text{Li}^+$  and interaction with the inner surface of the membrane.

For a quantitative analysis of the permeability of the open channels it is essential to know the current for a constant number of open channels as a function of membrane potentials. Because of gating processes which depend on membrane potential the peak inward current does not follow the condi-

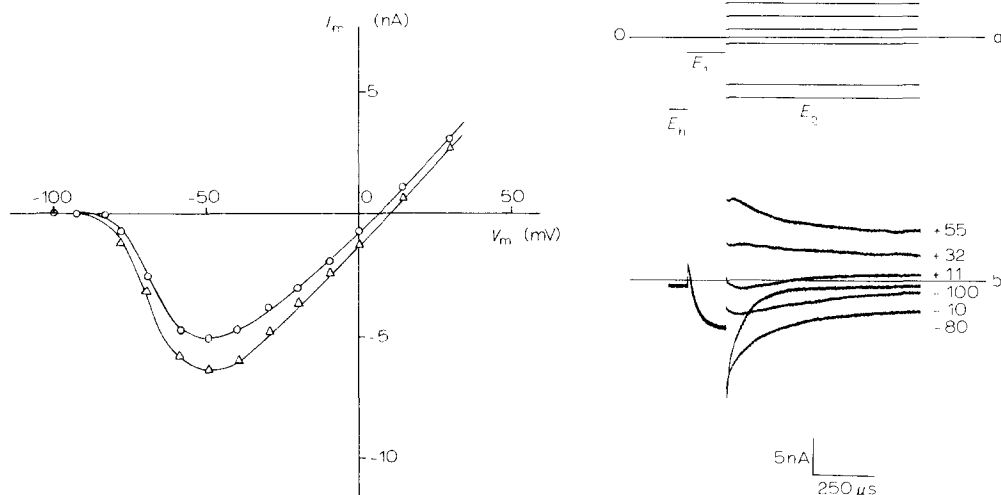


Fig. 5. Peak current-voltage relations for a node treated with  $10^{-4}$  g/ml aconitine in  $\text{Na}^+$ -Ringer (circles) and  $\text{Ti}^+$ -Ringer (triangles). Currents corrected for leakage and capacity. Node 43, temperature =  $22^\circ\text{C}$ .

Fig. 6. Measurement of "instantaneous" currents. (a) pulse programme for measuring "instantaneous" currents,  $E_h = -120$  mV,  $E_1 = -20$  mV, (b) currents associated with pulses  $E_1$  and  $E_2$  in  $\text{Na}^+$ -Ringer for a node treated with  $10^{-4}$  g/ml aconitine. Membrane potential during  $E_2$  are indicated on the right. Currents are not corrected for leakage and capacity. Node 61, temperature =  $14^\circ\text{C}$ .

tion of a constant number of open channels. This condition is fulfilled, however, for the so called "instantaneous" currents [13].

Fig. 6 shows the pulse program used for measuring instantaneous currents and tracings of the currents recorded with  $\text{Na}^+$ -Ringer. Currents measured at the beginning of test pulse  $E_2$ , regardless of its amplitude, correspond to the constant number of open channels which is attained at the end of pulse  $E_1$ .

The kinetic properties of ionic currents (associated with the first and second pulses) change little with cationic substitutions. It follows that the gating process and hence the number of open channels at the end of pulse  $E_1$ , does not change essentially.

When correcting the instantaneous currents for capacity currents, the observation that the ionic current associated with a negative pulse to  $-100$  mV decays exponentially was used. This exponential current was extrapolated to zero time and the difference between the current measured and the extrapolated curve were taken to represent capacitive current. When correcting for capacity current at other potentials the assumption was made that it is proportional to the voltage change  $E_2 - E_1$ .

Fig. 7 shows a family of instantaneous current-voltage relations for a node bathed in various Ringer's solutions made with  $\text{Cs}^+$ ,  $\text{K}^+$ ,  $\text{Li}^+$ ,  $\text{NH}_4^+$  and  $\text{Na}^+$ . It may be seen that the steepness of these curves decreases at more negative potentials and increases in the opposite direction. This result indicates a clear rectification of the outward current. Such rectification in the case of  $\text{Na}^+$ - and  $\text{NH}_4^+$ -Ringer's is unexpected, since  $\text{Na}^+$  and  $\text{NH}_4^+$  are more permeable through modified channels than the internal  $\text{K}^+$  and Goldman-Hodgkin-Katz equation [14,15] in such a case predicts rectification of the inward current.



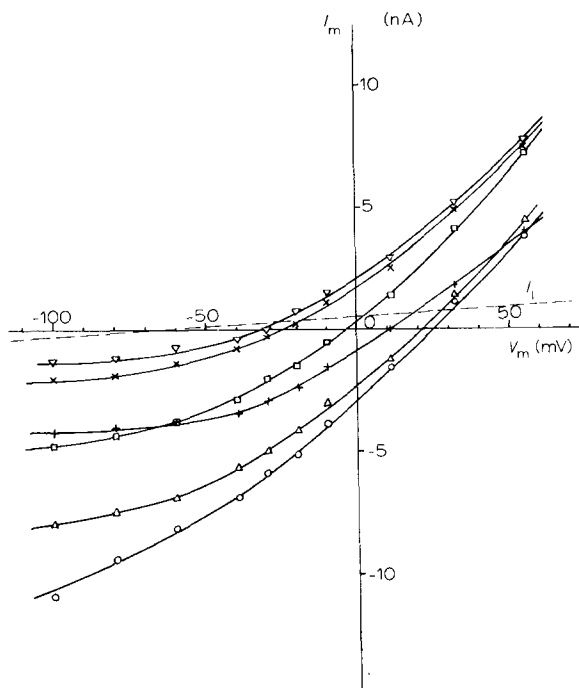


Fig. 7. "Instantaneous" current-voltage relations for a node treated with  $10^{-4}$  g/ml aconitine bathed in  $\text{NH}_4^+$ ,  $\text{K}^+$ ,  $\text{Li}^+$ ,  $\text{Rb}^+$ ,  $\text{Cs}^+$ ,  $\text{Na}^+$ -Ringers. Currents corrected for leakage and capacity. Node 61, temperature,  $14^\circ\text{C}$ .  $\circ$ ,  $\text{NH}_4^+$ ;  $\Delta$ ,  $\text{Na}^+$ ;  $+$ ,  $\text{Li}^+$ ;  $\square$ ,  $\text{K}^+$ ;  $\times$ ,  $\text{Rb}^+$ ;  $\nabla$ ,  $\text{Cs}^+$ .

The comparison of instantaneous and peak current-voltage relations indicates that the non-linearity of peak current-voltage relations at potentials more positive than  $-30$  mV is determined by the properties of open channels rather than by a change in the number as a result of activation and inactivation gating.

In Fig. 7 the current-voltage relation in  $\text{Li}^+$ -Ringer is less steep than it might be expected from the value of  $\Delta E_r^{\text{Li}}$ . This observation is an example that just changes in  $E_r$ ,  $\Delta E_r$ , are not sufficient to describe selectivity properties of channels: at least one more parameter (characterising the steepness of the curve) is needed. The slope of current-voltage curve near  $E_r$  ( $g_r$ ) is such a parameter. The average slopes of the instantaneous current-voltage relation in the test solution relative to that in  $\text{Na}^+$ -Ringer ( $g_r^i/g_r^{\text{Na}}$ ) were:  $1.14 \pm 0.05$ ,  $0.80 \pm 0.03$ ;  $0.67 \pm 0.12$ ;  $0.53 \pm 0.10$ ;  $0.53 \pm 0.06$  (mean  $\pm$  S.D.) for  $\text{NH}_4^+$ ,  $\text{K}^+$ ,  $\text{Rb}^+$ ,  $\text{Cs}^+$  and  $\text{Li}^+$ , respectively. Temperature does not affect  $g_r^i/g_r^{\text{Na}}$  in a noticeable manner.

In five experiments  $\text{Na}^+$ -Ringer was substituted by  $0.5$   $\text{Na}^+$ -Ringer. The average value of the relative slope was  $0.83 \pm 0.06$ , i.e. approximately as much as for  $\text{K}^+$ -Ringer. The average value of  $E_{r,2}^{\frac{1}{2}\text{Na}}$  was equal to  $-17.4 \pm 0.5$  mV; practically the same as that expected from the Nernst equation.

### Analysis and Discussion

Two models based on Eyring's theory have been proposed to describe ion transport through  $\text{Na}^+$ -channels: a three barrier model [1] and a four barrier

model [16]. The suggestion that the selectivity filter imposes the higher energy barrier is common for both models. In Hille's model the major barrier is  $G_{23}$  (using Hille's nomenclature). In Chizmadgev's model the major barrier is the central one. The difference between the highest barrier and the barriers which separate the potential wells from adjacent solutions results in a practically equilibrium distribution of ions between the wells and adjacent solutions.

The reversal potential for the current through a channel, at a given concentration of penetrating ions, depends on the height of the energy barrier in the channel, and in the case of a large difference between them, mainly on the highest barrier(s) [17]. Hence, the shift of  $E_r$  depends on the difference between the energies of the ions at the peak of the highest barrier.

As the distribution of ions between the external solution and that part of the channel representing an energy well is at equilibrium, changes in the slope of current-voltage curves caused by cationic substitution in external solution must be due to differences in the energy between the external well and the peak of the highest barrier for the various cations tested. Thus, in estimating this energy difference other details of the energy profile within the channel are not of great importance and the rather simple equation of the three barrier model [1] may be used. It is clear that for the description of the current-voltage relations over a wider range of membrane potentials more realistic models (for example such as Hille's model [16]) would be more adequate. However, for using such a model additional data are needed.

Let us write  $G_b^i$  as the energy levels of test ion at the peak of major barrier and  $G_w^i$  in external energy well. If we take the energy levels for  $\text{Na}^+$  as reference levels we obtain  $\Delta G_b^i = G_b^i - G_b^{\text{Na}}$  and  $\Delta G_w^i = G_w^i - G_w^{\text{Na}}$  for the test cations.

Substituting the values of the rate constants as exponential functions of the energy levels in the formula for the reversal potential 17 as calculated using the three barrier model [1] we have

$$\Delta G_b^i/RT = -\Delta E_r^i F/RT \quad (1),$$

where  $F$ ,  $R$ ,  $T$  have their usual meanings. The values of  $\Delta G_b^i$  calculated with Eqn. 1 are given in the upper half of Fig. 8 in  $RT$  units. In these calculations we neglected the dependence of  $\Delta E_r^i$  on temperature and substituted the average from all the experiments into Eqn. 1. Thus,  $\Delta G_b^i$  in Fig. 8 relates to a range of temperatures between 13 and 22°C.  $\Delta G_b^i$  for normal sodium channels are also presented in the figure. These values were calculated by substituting the average  $\Delta E_r^i$  from Hille's papers [11,12] into Eqn. 1. Besides,  $\Delta E_r^{\text{K}}$  values from three experiments ( $\text{Na}^+$ -Ringer was replaced by  $\text{K}^+$ -Ringer) from a previous paper [3], were used.

$\Delta G_b^i$  for  $\text{NH}_4^+$ ,  $\text{K}^+$ ,  $\text{Rb}^+$ ,  $\text{Cs}^+$  in modified  $\text{Na}^+$ -channels is smaller than in normal  $\text{Na}^+$ -channels. Differences between the values of  $\Delta G_b^i$  of normal and modified channels for  $\text{K}^+$ ,  $\text{Rb}^+$ ,  $\text{Cs}^+$  are equal to 1.8, 2.9 and 2.6  $RT$ , respectively. The main barrier to  $\text{NH}_4^+$  of modified channel is lower than that to  $\text{Na}^+$  ( $\Delta G_b^{\text{NH}_4} = -0.3 RT$ ) while in normal  $\text{Na}^+$ -channels  $\Delta G_b^{\text{NH}_4}$  is higher by 1.8  $RT$ .  $\Delta G_b^{\text{Tl}}$ , as well as  $\Delta G_b^{\text{NH}_4}$ , is negative and makes up about 0.1  $RT$ .

In as much as  $\text{NH}_4^+$  and  $\text{Tl}^+$  are larger than  $\text{Na}^+$  it may be suggested that

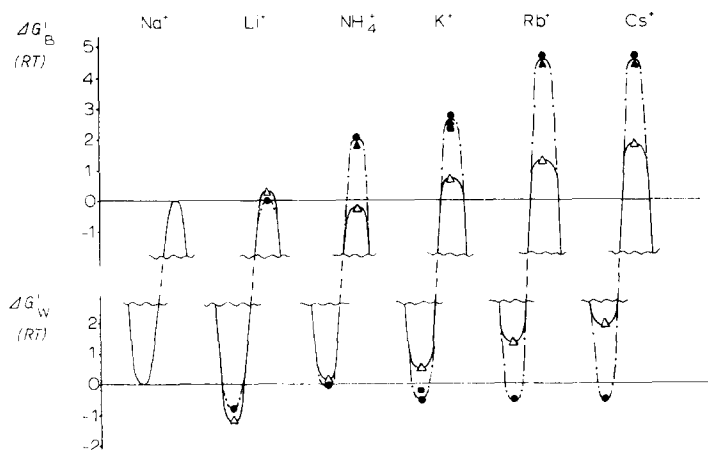


Fig. 8. Energy levels for  $\text{Li}^+$ ,  $\text{NH}_4^+$ ,  $\text{K}^+$ ,  $\text{Rb}^+$ ,  $\text{Cs}^+$  and  $\text{Na}^+$  in normal (filled symbols) and aconitine-modified (open symbols) channel. Open triangles, modified channel, three barrier model [1]; filled circles, data from [11,12], four barrier model [16]; filled triangles, data from [11,12], three barrier model [1]; filled squares, data from present work and ref. 3, three barrier model. Top: the energy of the ions at the peak of the major barrier; bottom: the energy of the ions in the external potential well. See text for details.

aconitine-modified sodium channel has a wider cross-section at its narrowest part.

$\Delta G_b^{\text{Li}}$  of modified channel makes up  $+0.2 RT$ , that is, a little more than the normal channel where  $\Delta G_b^{\text{Li}} < 0.1 RT$ .

Energy values at the peak of the highest barrier in normal  $\text{Na}^+$ -channels calculated with a four barrier model are listed in Table II of Hille's work [16].  $\Delta G_b^i$  calculated from these values are shown in Fig. 8. As may be seen they differ slightly from  $\Delta G_b^i$  calculated using Eqn. 1.

As to the changing in the absolute values of  $G_b^i$  caused by aconitine, the available data suggest that  $G_b^i$  decreases for  $\text{NH}_4^+$ ,  $\text{Tl}^+$ ,  $\text{K}^+$ ,  $\text{Rb}^+$ ,  $\text{Cs}^+$  and increases for  $\text{Na}^+$  and  $\text{Li}^+$ . But we feel that additional experimental data are needed.

The decrease of  $E_r^i$  and, consequently, of  $G_b^i$  for  $\text{K}^+$ ,  $\text{Rb}^+$  and  $\text{Cs}^+$  with the increase of temperature from  $13\text{--}14^\circ\text{C}$  to  $20\text{--}22^\circ\text{C}$ , indicates some flexibility of the structures involved due to which thermal motion blurs the perimeter of the channel.

To calculate the binding constants at the external potential well ( $K_i$ ), the following equation was used:

$$g_r^i/g_r^{\text{Na}} = \frac{1 + K_{\text{Na}}C_{\text{Na}}}{1 + K_iC_i} \cdot \exp \Delta E_r^i F/2RT \quad (2)$$

where  $C_{\text{Na}}$  and  $C_i$  are the activities of  $\text{Na}^+$  and test ions in external solution (for all ions the activity coefficient was assumed to be 0.78). This equation comes from formulae 17 and 18 of the three barrier model [1]. Strictly speaking Eqn. 2 is correct only when the membrane potential takes place at the central barrier. However,  $K_i$  and  $K_{\text{Na}}$  obtained in this way differ slightly from the corresponding figures found from other equations of the same model, which suggests a more realistic distribution of the potential.

$K_{Na}$  for modified channels was determined by substitution of  $g_r^{1/2 Na}/g_r^{Na}$  into Eqn. 2; it turned out to be  $4.8 \text{ M}^{-1}$ .

Further, substituting this value of  $K_{Na}$  and average values of  $g_r^i/g_r^{Na}$  and  $\Delta E_r^i$  into Eqn. 2 we obtained  $K_i$ . They proved to be 15.0, 5.1, 2.8, 1.2 and  $0.7 \text{ M}^{-1}$  for  $\text{Li}^+$ ,  $\text{NH}_4^+$ ,  $\text{K}^+$ ,  $\text{Rb}^+$  and  $\text{Cs}^+$ , respectively. From the slope of the current-voltage relation in  $\text{Ti}^+$ -Ringer (Fig. 5)  $K_{Ti}$  should be close to  $K_{NH_4}$ , that is about  $5 \text{ M}^{-1}$ .

To compute  $K_{Na}$  and  $K_K$  for the normal channel the results from four experiments with  $1/5 \text{ Na}^+$ -Ringer in place of the normal concentration (see Materials and Methods) and from three experiments with  $\text{K}^+$ -Ringer in place of  $\text{Na}^+$ -Ringer from a previous work [3] were used. It gave  $K_{Na} = 2.8 \text{ M}^{-1}$  and  $K_K = 3.3 \text{ M}^{-1}$  for normal sodium channels. According to Hille's work [16]  $K_{Na} = 2.7 \text{ M}^{-1}$ ,  $K_{Li} = 6 \text{ M}^{-1}$ ,  $K_{NH_4} = 2.7 \text{ M}^{-1}$ ,  $K_K = K_{Rb} = K_{Cs} = 4.5 \text{ M}^{-1}$ .

The comparison of the binding constants for normal and modified channels shows that the energy of binding of  $\text{Na}^+$ ,  $\text{Li}^+$ ,  $\text{NH}_4^+$  in modified channels is greater than in the normal ones. As for the binding energies of  $\text{K}^+$ ,  $\text{Rb}^+$ ,  $\text{Cs}^+$  and  $\text{Ti}^+$  they are smaller than in the normal  $\text{Na}^+$ -channel.

Different binding energies in normal and modified channels are presented in the lower half of Fig. 8, which shows  $\Delta G_w^i$  for both types of channels.  $\Delta G_w^i$  (in  $RT$  units) was calculated according to

$$\Delta G_w^i = -\ln K_i/K_{Na} \quad (3)$$

Summarising the results we conclude that modification of  $\text{Na}^+$ -channels by aconitine leads to drastic changes in the energy profile. This suggests that certain structural rearrangements of that part of the  $\text{Na}^+$ -channel determining its selective properties take place.

According to the hypothesis that the "selective filter" is also the receptor for tetrodotoxin [18,19] one might expect changes in the equilibrium dissociation constant between receptor and tetrodotoxin after treatment with aconitine. This constant has not changed [3]. Thus, the structures of tetrodotoxin-receptor and "selective filter" do not coincide. Tetrodotoxin binds, apparently, just near the outer surface of the membrane. The absence of the voltage dependence of tetrodotoxin block in  $\text{Na}^+$ -channels [20] is also an argument in favour of this assumption.

The effect on the gating mechanism of  $\text{Na}^+$ -channels was the first effect discovered for aconitine; it manifests itself in a shift of the conductance-voltage curve towards more negative potentials. The acceleration of development of the aconitine effect with repetitive depolarization suggests that the "open" configuration of gates is more favourable for interaction with aconitine.

Investigations on the effects of aconitine on both selectivity properties and gating processes in  $\text{Na}^+$ -channels would be of interest for understanding structural inter-relations between different parts of the channel. Our preliminary observations indicate that aconitine brings about a shift in the voltage range of "gating current" activation. A detailed study of the gating processes in the presence of aconitine will be the subject of a later investigation.

#### Acknowledgement

We wish to thank Dr. V.V. Malev for useful discussion.

## References

- 1 Chizmadgev, Yu.A., Khodorov, B.I. and Aityan, S.Kh. (1974) *Bioelectrochem. Bioenerg.* 1, 301—312
- 2 Schmidt, H. and Schmitt, O. (1974) *Pflügers Arch.* 349, 133—148
- 3 Mozhayeva, G.N., Naumov, A.P. and Negulyaev, Yu.A., (1976) *Neurophysiologiya* 8, 152—161
- 4 Nonner, W. (1969) *Pflügers. Arch.* 309, 176—192
- 5 Lonsky, A.V., Ilyin, V.I. and Malov, A.M. (1972) *Physiol. Zhur. U.S.S.R.* 58, 136—138
- 6 Mozhayev, G.A. (1970) *Tsitologiya* 12, 930—937
- 7 Dodge, F.A. and Frankenhauser, B. (1958) *J. Physiol.* 143, 76—90
- 8 Koppenhöfer, E. and Vogel, W. (1969) *Pflügers. Arch.* 313, 361—380
- 9 Mozhayeva, G.N. and Naumov, A.P. (1972) *Biochim. Biophys. Acta* 29, 248—255
- 10 Chandler, W.K. and Meves, H. (1965) *J. Physiol.* 180, 788—820
- 11 Hille, B. (1971) *J. Gen. Physiol.* 58, 599—612
- 12 Hille, B. (1972) *J. Gen. Physiol.* 59, 637—658
- 13 Hodgkin, A.L. and Huxley, A.F. (1952) *J. Physiol.* 116, 449—472
- 14 Goldman, D.E. (1943) *J. Gen. Physiol.* 27, 37—60
- 15 Hodgkin, A.L. and Katz, B. (1949) *J. Physiol.* 108, 37—77
- 16 Hille, B. (1975) *J. Gen. Physiol.* 66, 535—560
- 17 Läuger, F. (1973) *Biochim. Biophys. Acta* 311, 423—442
- 18 Kao, C.Y. and Nishiyama, A. (1965) *J. Physiol.* 180, 50—66
- 19 Hille, B. (1975) *Biophys. J.* 15, 615—619
- 20 Hille, B. (1968) *J. Gen. Physiol.* 51, 199—219